



Cite this: RSC Adv., 2017, 7, 24040

Visible light-induced PET-RAFT polymerization of methacrylates with novel organic photocatalysts

Kai Tu, Tianchi Xu, Lifen Zhang,* Zhenping Cheng * and Xiulin Zhu

Light-emitting diode (LED) technology in the visible spectrum holds great promise for photopolymerization because of its characteristic virtues such as low energy consumption, no ozone release, low heat generation, simple and safe operation, high performance, etc. In this work, two organic agents, 4-methoxybenzaldehyde (PC1) and 2,4,6-tri-(*p*-methoxyphenyl) pyrylium tetrafluoroborate (PC2), were employed as the photocatalysts for the photoinduced electron transfer-reversible addition-fragmentation chain transfer (PET-RAFT) polymerization under irradiation of various LED lights (purple, blue and white LEDs) at room temperature, using methyl methacrylate (MMA) as the model monomer and typical 2-cyanoprop-2-yl 1-dithionaphthalate (CPDN) as the RAFT agent. It has been found that the polymerization could be carried out smoothly with a wide range of wavelengths of visible light and could be extended to other methacrylates such as ethyl methacrylate (EMA) and *n*-butyl methacrylate (*n*-BMA). In addition, the "living" feature of this polymerization system was demonstrated by its polymerization kinetics and was confirmed by a chain-extension experiment.

Received 16th March 2017

Accepted 23rd April 2017

DOI: 10.1039/c7ra03103c

rsc.li/rsc-advances

1. Introduction

Compared with traditional polymerization methods, controlled/living radical polymerization (LRP) has advantages of synthesizing well-designed polymeric materials with pre-determined molecular weight, narrow weight distribution and diverse architectures. Thanks to the effort of researchers, great achievements in the development of LRP methods have been made. Different strategies to modulate the balance between dormant and activate species have been found in recent years, such as nitroxide-mediated radical polymerization (NMP),¹ atom transfer radical polymerization (ATRP),² and reversible addition-fragmentation chain transfer (RAFT) polymerization.³

It is well known that various physical and chemical stimuli can be used to control the reversible activation of dormant species in LRP.⁴ For example, Matyjaszewski and co-workers successfully controlled the initiation and growth steps of LRP by exploiting the unique aspects of electro-chemistry to control the ratio of activator to deactivator in ATRP.^{4(a)} UV irradiation was also used to develop a LRP including iniferter polymerization.⁵ Unfortunately, UV irradiation would lead to the decomposition of dithioesters in the process of RAFT polymerization.^{3(f)} However, as a more environmentally friendly

external stimulus, light-emitting diodes (LED) in the visible spectrum is the most ideal stimulus due to its characteristic virtues such as low energy consumption, no ozone release, low heat generation, simple and safe operation, high performance. Now it has been successfully used in various LRP methods with controlled molecular and narrow molecular weight distribution under mild conditions.⁶

On the other hand, since Hawker and co-workers developed a kind of transition metal photoredox catalyst (e.g., fac-[Ir(ppy)₃]) for photoinduced ATRP,⁷ Boyer and co-workers established a highly efficient photoinduced electron transfer RAFT (PET-RAFT) polymerization using this kind of metal photoredox catalysts.⁸ Frustratingly, the resultant polymers are easily contaminated by the transition metal catalyst, and therefore limited its application fields (e.g., electronic materials) significantly. Therefore, organic photocatalyst is highly promising to solve the problem of PET-RAFT mentioned above. Now, some organic photocatalysts, such as methylene blue, fluorescein, rhodamine 6G, Nile red, eosin Y, porphyrin compounds, chlorophyll a (Chl a), and pheophorbide, were explored.⁹ In order to enrich the library of organic photocatalyst, in this work, by combination of both advantages of visible LED lights and PET-RAFT polymerization, the commercially available organic catalyst 4-methoxybenzaldehyde (PC1) and the synthesized 2,4,6-tri-(*p*-methoxyphenyl) pyrylium tetrafluoroborate (PC2) were used as the organic photocatalyst for the PET-RAFT polymerization of methacrylates under irradiation of visible LED lights at room temperature. The effect of solvent and wavelength of LED lights and polymerization kinetics was studied in detail.

Suzhou Key Laboratory of Macromolecular Design and Precision Synthesis, Jiangsu Key Laboratory of Advanced Functional Polymer Design and Application, State and Local Joint Engineering Laboratory for Novel Functional Polymeric Materials, Department of Polymer Science and Engineering, College of Chemistry, Chemical Engineering and Materials Science, Soochow University, Suzhou 215123, China. E-mail: chengzhenping@suda.edu.cn; zhanglifen@suda.edu.cn; Fax: +86-512-65882787



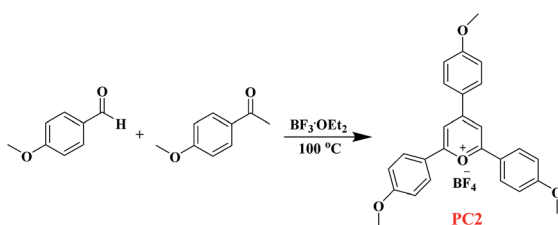
2. Experimental section

2.1. Materials

Monomers, methyl methacrylate (MMA, 99%) purchased from Shanghai Chemical Reagents Co. Ltd. (Shanghai, China), ethyl methacrylate (EMA, 98%) and *n*-butyl methacrylate (*n*-BMA, 99%) purchased from TCI (Shanghai, China) were removed the inhibitor by passing through a neutral alumina column before use. The RAFT agent 2-cyanoprop-2-yl 1-dithionaphthalate (CPDN) was prepared according to the method reported by the literature.¹⁰ Tetrahydrofuran (THF, analytical reagent) purchased from Nanjing Chemical Reagent Co. 4-Methoxybenzaldehyde (PC1) and 4'-methoxyacetophenone were purchased from Univ-bio (Shanghai, China). Ethyl ether boron fluoride ($\text{BF}_3 \cdot \text{Et}_2\text{O}$) was purchased from Innochem (Beijing, China). Toluene (analytical reagent), anisole (analytical reagent), *N,N*-dimethylformamide (DMF), 1,4-dioxane (analytical reagent), acetone (analytical reagent), dimethyl sulfoxide (DMSO), *N,N*-dimethylacetamide (DMAc, analytical reagent) were purchased from Chinasun Specialty Products Co. Ltd. and used as received unless mentioned.

2.2. Synthesis of 2,4,6-tri(*p*-methoxyphenyl) pyrylium tetrafluoroborate (PC2)

The synthetic route of PC2 is shown in Scheme 1. Details are as follows: to a flask containing 4-methoxybenzaldehyde (6.1 mL, 50.3 mmol, 1 equiv.) and *p*-acetylanisole (15.07 g, 100.4 mmol, 2 equiv.) was added $\text{BF}_3 \cdot \text{Et}_2\text{O}$ (15.0 mL, 121.5 mmol, 2.4 equiv.) dropwise over 5 min. The solution was placed in an oil bath set to 100 °C for 2 h. After cooled to room temperature, the crude material was diluted with acetone (200 mL) and Et_2O (250 mL)



Scheme 1 The synthetic pathway of organic photocatalyst 2,4,6-tri(*p*-methoxyphenyl) pyrylium tetrafluoroborate (PC2).

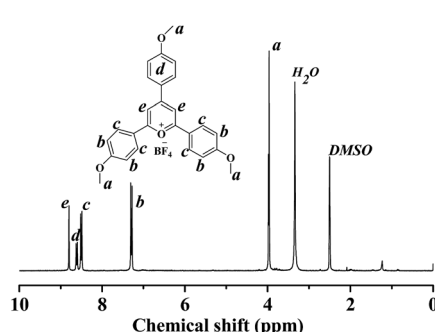


Fig. 1 ^1H NMR of the organic photocatalyst (PC2).

and filtered to give a rust-colored solid. The solids were washed with warm acetone (175 mL) and dried under vacuum to give the pyrylium tetrafluoroborate as an orange solid (5.01 g, 20% of yield). The structure of PC2 was analysed by ^1H NMR spectroscopy (Fig. 1), and its spectral matched that previously reported.¹¹

2.3. Typical procedures for PET-RAFT polymerization

A typical polymerization procedure with the molar ratio of $[\text{MMA}]_0 : [\text{PC1}]_0 : [\text{CPDN}]_0 = 400 : 50 : 1$ was described as follows. A mixture was obtained by adding CPDN (6.4 mg), MMA (1.0 mL), PC1 (0.14 mL), and solvent (DMAc, 0.5 mL) to a clean ampoule with a stir bar. The mixture was thoroughly bubbled with argon for 20 min to eliminate the dissolved oxygen, and then the ampoule was flame-sealed and irradiated under LED light with stirring at room temperature (25 °C), which was kept by a fanning. After the desire polymerization time, the ampoule was opened and the mixture was diluted by THF. After precipitation with plenty of petroleum ether in a glass, and standing overnight, it was filtered and dried in a vacuum oven at 40 °C until constant weight. The monomer conversion was determined by gravimetrically. The other procedures for PET-RAFT polymerization of MMA using PC2 as the organic photocatalyst were similar as that as described above.

2.4. Characterization

The number-average molecular weight ($M_{n,\text{GPC}}$) and molecular weight distribution (M_w/M_n) of the resultant polymers were determined by using a TOSOH HLC-8320 gel permeation chromatograph (GPC) equipped with a refractive-index detector (TOSOH), using TSKgel guardcolumn SuperMP-N (4.6 × 20 mm) and two TSKgel SupermultiporeHZ-N (4.6 × 150 mm) with measurable molecular weights ranging from 5×10^2 to $5 \times 10^5 \text{ g mol}^{-1}$. THF was used as the eluent at a flow rate of 0.6 mL min⁻¹ and 40 °C. GPC samples were injected using a TOSOH plus autosampler and calibrated with PMMA standards purchased from TOSOH. ^1H NMR spectra were recorded on Bruker 300 MHz nuclear magnetic resonance (NMR) instrument using CDCl_3 as the solvent and tetramethylsilane (TMS) as the internal standard at ambient temperature.

3. Results and discussion

3.1. Effect of solvent on the polymerization catalyzed by PC1

Firstly, we investigated the commercially available 4-methoxybenzaldehyde (PC1) photocatalyst¹² for this PET-RAFT polymerization system for the first time. Subsequently, the effect of solvent including toluene, anisole, 1,4-dioxane, DMAc, and DMF on the PET-RAFT polymerization were studied under irradiation of white LED light at room temperature, and the results are shown in Table 1. It can be seen that all the polymerizations were carried out smoothly and that relatively faster polymerization rate was observed in more polar solvents (e.g., DMAc, DMF) due to its basicity.¹² Taking into account the molecular weight and molecular weight distribution of the



Table 1 Effect of solvent on the PET-RAFT polymerization^a

Entry	Solvent	Conv. (%)	$M_{n,\text{th}}^b$ (g mol ⁻¹)	$M_{n,\text{GPC}}$ (g mol ⁻¹)	M_w/M_n
1	None	20.6	8200	13 500	1.27
2	Toluene	16.7	6700	12 700	1.26
3	Anisole	22.3	8900	15 600	1.24
4	DMF	27.6	11 000	16 300	1.62
5	DMAc	24.4	9760	16 610	1.21

^a Polymerization condition: $R = [\text{MMA}]_0 : [\text{PC1}]_0 : [\text{CPDN}]_0 = 400 : 50 : 1$, $V_{\text{MMA}} = 1.0$ mL, $m_{\text{CPDN}} = 6.4$ mg, $V_{\text{PC1}} = 0.14$ mL; temperature = 25 °C, $V_{\text{solvent}} = 0.5$ mL, under irradiation of white LED ($\lambda_{\text{max}} = 440, 540$ nm, 1.2 mW cm⁻²), time = 60 h. ^b $M_{n,\text{th}} = ([\text{M}]_0/[\text{CPDN}]_0) \times M_{w,\text{MMA}} \times \text{conv.}\%$.

Table 2 Effect of the wavelength of LED on the PET-RAFT polymerization^a

Entry	Time (h)	Conv. (%)	$M_{n,\text{th}}^e$ (g mol ⁻¹)	$M_{n,\text{GPC}}$ (g mol ⁻¹)	M_w/M_n
1 ^b	48	13.0	5200	12 200	1.32
2 ^b	72	56.6	22 600	30 600	1.16
3 ^c	48	49.2	19 700	25 000	1.23
4 ^c	72	95.7	38 200	45 300	1.26
5 ^d	48	53.5	21 400	27 400	1.11
6 ^d	72	96.6	38 600	46 400	1.15

^a Polymerization condition: $R = [\text{MMA}]_0 : [\text{PC1}]_0 : [\text{CPDN}]_0 = 400 : 50 : 1$, $V_{\text{MMA}} = 1.0$ mL, $V_{\text{PC1}} = 0.14$ mL, $m_{\text{CPDN}} = 6.4$ mg, $V_{\text{DMAc}} = 0.5$ mL, temperature = 25 °C. ^b White LED ($\lambda_{\text{max}} = 440, 540$ nm, 1.2 mW cm⁻²). ^c Blue LED ($\lambda_{\text{max}} = 464$ nm, 0.8 mW cm⁻²). ^d Purple LED ($\lambda_{\text{max}} = 391$ nm, 0.8 mW cm⁻²). ^e $M_{n,\text{th}} = ([\text{M}]_0/[\text{CPDN}]_0) \times M_{w,\text{MMA}} \times \text{conv.}\%$.

resultant polymers, DMAc (entry 5 in Table 1) as the solvent additionally preferred to be used.

3.2. Effect of the wavelength of LED and the amount of organic photocatalyst on the polymerization

In order to investigate the effect of wavelength of LED on the PET-RAFT polymerization at room temperature, we kept the optimized polymerization conditions constant and changed the

Table 3 Effect of the amount of organic photocatalyst on the PET-RAFT polymerization^a

Entry	R	Conv. (%)	$M_{n,\text{th}}^b$ (g mol ⁻¹)	$M_{n,\text{GPC}}$ (g mol ⁻¹)	M_w/M_n
1	400 : 20 : 1	30.2	12 100	19 500	1.25
2	400 : 30 : 1	32.3	12 900	20 400	1.24
3	400 : 40 : 1	43.1	17 200	25 500	1.18
4	400 : 50 : 1	53.7	21 500	28 200	1.11
5	400 : 200 : 1	63.7	25 500	38 500	1.16

^a Polymerization condition: $R = [\text{MMA}]_0 : [\text{PC1}]_0 : [\text{CPDN}]_0$, $V_{\text{MMA}} = 1.0$ mL, $V_{\text{PC1}} = 0.14$ mL, $m_{\text{CPDN}} = 6.4$ mg, $V_{\text{DMAc}} = 0.5$ mL, temperature = 25 °C, white LED ($\lambda_{\text{max}} = 440, 540$ nm, 1.2 mW cm⁻²), time = 72 h.

^b $M_{n,\text{th}} = ([\text{M}]_0/[\text{I}]_0) \times M_{w,\text{MMA}} \times \text{conv.}\%$.

wavelength of LED (purple LED, blue LED and white LED). As shown in Table 2, the polymerization could be carried out successfully in all cases although the polymerization rate changed with the wavelength, which increased with decrease of wavelength. For example, the monomer conversion was 56.6%, 95.7% and 96.6% for the case under irradiation of purple, blue and white LED light, respectively. This is contributed to the fact that higher energy for the shorter wavelength of LED light. In addition, the effect of the amount of PC1 on the polymerization was also investigated, and the results are shown in Table 3. It can be seen that increasing the amount of catalyst enhanced the polymerization rate as expected.

3.3. Kinetics of the polymerization catalyzed by PC1 under irradiation of different light

In order to further investigate the detailed polymerization behaviors under various wavelength of LED, the polymerization kinetics of MMA was conducted with the molar ratio of $[\text{MMA}]_0 : [\text{PC1}]_0 : [\text{CPDN}]_0 = 400 : 50 : 1$ under irradiation of white LED, blue LED and purple LED, respectively. Fig. 2(A) shows the kinetic plots of $\ln([\text{M}]_0/[\text{M}])$ versus time. The first-order polymerization kinetics was observed in all cases, which indicating a constant concentration of propagating radicals during these polymerization processes. It should be noted that induction period of the polymerization under blue LED (17 h) and purple LED (15 h) is much shorter than that under white

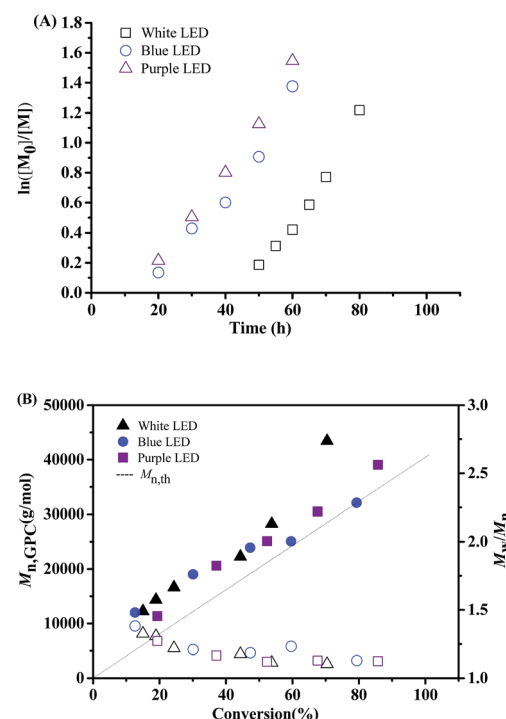


Fig. 2 $\ln([\text{M}]_0/[\text{M}])$ as a function of time (A) and evolution of number-average molecular weight ($M_{n,\text{GPC}}$) and molecular weight distribution (M_w/M_n) versus conversion (B) under irradiation of different LED lights. Polymerization conditions: $R = [\text{MMA}]_0 : [\text{PC1}]_0 : [\text{CPDN}]_0 = 400 : 50 : 1$, $V_{\text{MMA}} = 1.0$ mL, $V_{\text{PC1}} = 0.14$ mL, $m_{\text{CPDN}} = 6.4$ mg, $V_{\text{DMAc}} = 0.5$ mL, temperature = 25 °C.



LED (46 h). Fig. 2(B) shows the evolution of $M_{n, \text{GPC}}$ and M_w/M_n versus monomer conversion, and it can be seen that the molecular weights increased linearly with monomer conversion while keeping narrow molecular weight distributions. All these results indicated the “living” features of the PET-RAFT polymerization at room temperature.

3.4. PET-RAFT polymerization catalyzed by PC2

As reported by the reference, 2,4,6-tri-(*p*-methoxyphenyl) pyrrolium tetrafluoroborate (PC2) is a good organic photocatalyst for cationic polymerization.¹³ In this work, we employed it as the photocatalyst for the PET-RAFT polymerization, and the results are shown in Table 4. The polymerization could be carried out under irradiation of white, blue and purple LED lights. In order to investigate the potential interference with classical photo-RAFT (iniferter) initiation,¹⁴ we also carried out the control experiments in the absence of photocatalyst PC2 under blue and purple LED lights. The results are listed in entries 8–11 in Table 4. It can be seen that an enhanced polymerization rate for the photocatalyst was observed. For example, monomer conversion increased from 39.5% (entry 11) in the absence of photocatalyst to 59.2% (entry 7) for the case of photocatalyst PC2 under purple LED light. These results indicated that classical photoRAFT (iniferter) initiation actually existed in the polymerization system; however, the addition of photocatalyst could enhance the polymerization rate significantly. From the GPC results, the resultant polymers are well-controlled with narrow molecular weight distributions except for that (entries 2 and 3) under irradiation of white LED light, indicating that PC2 can also serve as a good candidate for the PET-RAFT polymerization. In order to explain the experimental phenomenon, we tested the absorption spectrum of PC2 (Fig. 3). It can be seen that the emission wavelengths of purple and blue LED lights are within the range of absorption wavelength of PC2, which facilitated to achieve high efficiency of photocatalyst.¹⁵

Table 4 Effect of the wavelength of LED on the polymerization in the presence/absence of PC2

Entry	Time (h)	Conv. (%)	$M_{n,\text{th}}^f$ (g mol ⁻¹)	$M_{n,\text{GPC}}$ (g mol ⁻¹)	M_w/M_n
1 ^a	24	—	—	—	—
2 ^a	48	9.1	3600	3900	1.54
3 ^a	72	35.5	14 200	21 300	1.62
4 ^b	24	23.0	9200	15 100	1.35
5 ^b	48	47.3	18 900	26 800	1.36
6 ^c	24	30.1	12 000	19 500	1.24
7 ^c	48	59.2	23 700	30 000	1.23
8 ^d	24	12.7	5400	8100	1.15
9 ^d	48	34.2	14 000	18 900	1.26
10 ^e	24	17.4	7200	13 600	1.24
11 ^e	48	39.5	16 100	23 300	1.29

Polymerization condition: ^{a,b,c} $R = [\text{MMA}]_0 : [\text{PC2}]_0 : [\text{CPDN}]_0 = 400 : 0.5 : 1$, $V_{\text{MMA}} = 1.0 \text{ mL}$, $m_{\text{PC2}} = 5.7 \text{ mg}$, $m_{\text{CPDN}} = 6.4 \text{ mg}$, $V_{\text{DMAc}} = 0.5 \text{ mL}$. ^aWhite LED ($\lambda_{\text{max}} = 440, 540 \text{ nm}$, 1.2 mW cm^{-2}). ^{b,d}Blue LED ($\lambda_{\text{max}} = 464 \text{ nm}$, 0.8 mW cm^{-2}). ^{c,e}Purple LED ($\lambda_{\text{max}} = 391 \text{ nm}$, 0.8 mW cm^{-2}). ^{d,e} $R = [\text{MMA}]_0 : [\text{CPDN}]_0 = 400 : 1$, $V_{\text{MMA}} = 1.0 \text{ mL}$, $m_{\text{CPDN}} = 6.4 \text{ mg}$, $V_{\text{DMAc}} = 0.5 \text{ mL}$. ^f $M_{n,\text{th}} = ([M]_0/[CPDN]_0) \times M_{w,\text{MMA}} \times \text{conv.}$. ^{a–e}Temperature = 25 °C.

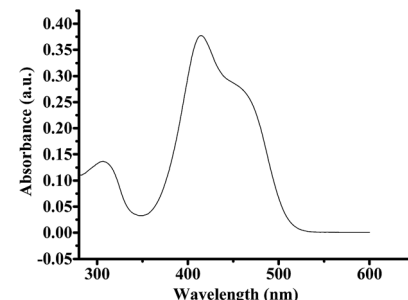


Fig. 3 UV-vis absorption spectrum of the synthetic photocatalyst PC2.

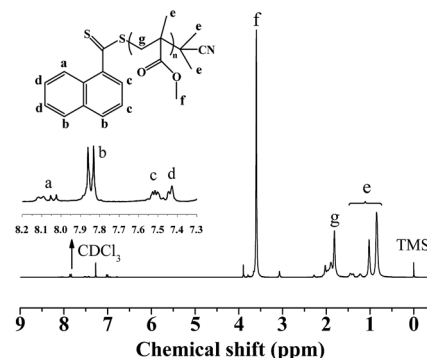


Fig. 4 ¹H NMR spectrum of the resultant PMMA catalysed by PC1 with CDCl_3 as solvent.

3.5. End analysis, chain extension and versatility for other monomers

The chain-end of the resultant PMMA, catalysed by PC1, was analyzed by ¹H NMR spectroscopy, as shown in Fig. 4. The chemical shifts at $\delta = 0.8\text{--}1.2 \text{ ppm}$ were corresponded to methyl protons of the PMMA repeat units and naphthalene moieties in CPDN; and the chemical shifts at $\delta = 7.4\text{--}8.1 \text{ ppm}$ were corresponded to the aromatic protons of the naphthalene units in CPDN,¹⁶ which indicated that the CPDN moieties were

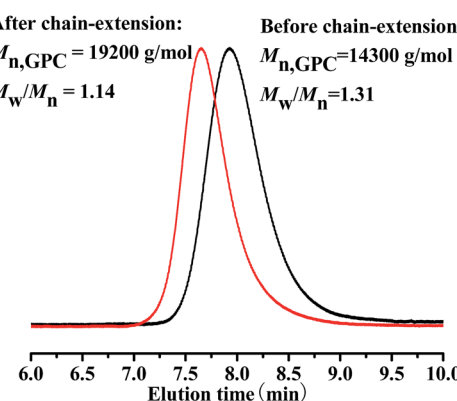


Fig. 5 GPC traces of before and after chain extension using random polymer PMMA as the macro-RAFT agent ($M_{n,\text{GPC}} = 14 300 \text{ g mol}^{-1}$, $M_w/M_n = 1.31$). Polymerization conditions: $[\text{MMA}]_0 : [\text{PC1}]_0 : [\text{CPDN}]_0 = 400 : 50 : 1$, $V_{\text{MMA}} = 1.0 \text{ mL}$, $V_{\text{PC1}} = 0.14 \text{ mL}$, temperature = 25 °C, $V_{\text{DMAc}} = 0.5 \text{ mL}$, under irradiation of purple LED (391 nm, 0.8 mW cm^{-2}).



Table 5 Versatility for other monomers catalyzed by PC1 and PC2^a

Entry	Catalyst	Monomer	Conv. (%)	$M_{n,\text{th}}^d$ (g mol ⁻¹)	$M_{n,\text{GPC}}$ (g mol ⁻¹)	M_w/M_n
1 ^b	PC1	EMA	44.1	20 100	26 800	1.24
2 ^b	PC1	<i>n</i> -BMA	39.7	22 500	30 700	1.27
3 ^c	PC2	EMA	46.3	21 100	28 300	1.22
4 ^c	PC2	<i>n</i> -BMA	43.6	24 800	31 400	1.13

^a Polymerization conditions: under irradiation of blue LED ($\lambda_{\text{max}} = 464$ nm, 0.8 mW cm⁻²), temperature = 25 °C, time = 48 h. ^b $R = [\text{monomer}]_0 : [\text{PC1}]_0 : [\text{CPDN}]_0 = 400 : 50 : 1$. ^c $R = [\text{monomer}]_0 : [\text{PC2}]_0 : [\text{CPDN}]_0 = 400 : 0.5 : 1$. ^d $M_{n,\text{th}} = ([M]_0 / [\text{CPDN}]_0) \times M_{w,\text{MMA}} \times \text{conv.}\%$.

attached to the polymer chain-end successfully. In order to further verify the end functionality of the resultant PMMA, a chain extension experiment was conducted with fresh MMA monomer using PMMA ($M_{n,\text{GPC}} = 14\,300$ g mol⁻¹, $M_w/M_n = 1.31$) as the macro-RAFT agent. From Fig. 5, it was found that the $M_{n,\text{GPC}}$ increased to 19 200 g mol⁻¹ ($M_w/M_n = 1.14$) after chain extension. Based on the above experimental results, we can draw the conclusion that polymeric product has a high degree of chain-end functionality, further verifying the “living” features of this polymerization system.

In order to investigate the versatility of the polymerization system, EMA and *n*-BMA were used as the monomers to conduct PET-RAFT polymerization. The results are shown in Table 5. It can be seen that the polymerization system is also suitable for EMA and *n*-BMA, verifying by the controlled molecular weights and molecular weight distributions of the resultant polymers in the cases of both PC1 and PC2.

4. Conclusions

The two novel organic agents 4-methoxybenzaldehyde and 2,4,6-tri-(*p*-methoxyphenyl) pyrylium tetrafluoroborate were explored as the photocatalysts for the PET-RAFT polymerization of methacrylates (e.g., MMA, EMA and *n*-BMA) under irradiation of LED lights successfully for the first time. Through the experiments, we investigated the effect of the types of solvents and lights on the polymerization and screened the optimal polymerization conditions. It was found that DMAc as the solvent can improve the polymerization rate and controllability due to the better solubility for the polymerization system. In addition, the polymerization was well-controlled under irradiation of blue and purple LED lights.

Acknowledgements

The financial support from the Nature Science Key Basic Research of Jiangsu Province for Higher Education (No. 16KJA150003), the National Natural Science Foundation of China (No. 21674071) and the Project Funded by the Priority Academic Program Development of Jiangsu Higher Education Institutions (PAPD) is gratefully acknowledged.

Notes and references

1 (a) M. K. Georges, R. P. N. Veregin, P. M. Kazmaier and G. K. Hamer, *Macromolecules*, 1993, **26**, 2987–2988; (b)

C. J. Hawker, A. W. Bosman and E. Harth, *Chem. Rev.*, 2001, **101**, 3661–3688; (c) V. Sciannamea, R. Jérôme and C. Detrembleur, *Chem. Rev.*, 2008, **108**, 1104–1126; (d) J. Nicolas, Y. Guillaneuf, C. Lefay, D. Bertin, D. Gigmes and B. Charleux, *Prog. Polym. Sci.*, 2013, **38**, 63–235; (e) J. C. Scaiano, T. J. Connolly, N. Mohtat and C. N. Pliva, *Can. J. Chem.*, 1997, **75**, 92–97; (f) S. Hu, J. H. Malpert, X. Yang and D. C. Neckers, *Polymer*, 2000, **41**, 445–452; (g) A. Goto, J. C. Scaiano and L. Marette, *Photochem. Photobiol. Sci.*, 2007, **6**, 833–835; (h) D. L. Versace, Y. Guillaneuf, D. Bertin, J. P. Fouassier, J. Lalevee and D. Gigmes, *Org. Biomol. Chem.*, 2011, **9**, 2892–2898; (i) J. Morris, S. Telitel, K. E. Fairfull-Smith, S. E. Bottle, J. Lalevee, J. L. Clement, Y. Guillaneuf and D. Gigmes, *Polym. Chem.*, 2015, **6**, 754–763. 2 (a) M. Kato, M. Kamigaito, M. Sawamoto and T. Higashimura, *Macromolecules*, 1995, **28**, 1721–1723; (b) J. S. Wang and K. Matyjaszewski, *J. Am. Chem. Soc.*, 1995, **117**, 5614–5615; (c) K. Matyjaszewski and J. H. Xia, *Chem. Rev.*, 2001, **101**, 2921–2990; (d) M. Kamigaito, T. Ando and M. Sawamoto, *Chem. Rev.*, 2001, **101**, 3689–3746; (e) L. J. Bai, L. F. Zhang, Z. P. Cheng and X. L. Zhu, *Polym. Chem.*, 2012, **3**, 2685–2697; (f) W. W. He, H. J. Jiang, L. F. Zhang, Z. P. Cheng and X. L. Zhu, *Polym. Chem.*, 2013, **4**, 2919–2938; (g) Z. B. Guan and B. Smart, *Macromolecules*, 2000, **33**, 6904–6906; (h) X. W. Jiang, J. Wu, L. F. Zhang, Z. P. Cheng and X. L. Zhu, *Macromol. Rapid Commun.*, 2014, **35**, 1879–1885; (i) M. Ciftci, M. A. Tasdelen and Y. Yagci, *Polym. Chem.*, 2014, **5**, 600–606; (j) X. Pan, N. Malhotra, J. Zhang and K. Matyjaszewski, *Macromolecules*, 2015, **48**, 6948–6954; (k) X. W. Jiang, L. F. Zhang, Z. P. Cheng and X. L. Zhu, *Macromol. Rapid Commun.*, 2016, **37**, 1337–1343; (l) B. J. Zhang, L. Yao, X. D. Liu, L. F. Zhang, Z. P. Cheng and X. L. Zhu, *ACS Sustainable Chem. Eng.*, 2016, **4**, 7066–7073; (m) X. D. Liu, L. F. Zhang, Z. P. Cheng and X. L. Zhu, *Polym. Chem.*, 2016, **7**, 689–700; (n) Z. C. Huang, Y. Gu, X. D. Liu, L. F. Zhang, Z. P. Cheng and X. L. Zhu, *Macromol. Rapid Commun.*, 2016, DOI: 10.1002/marc.201600461. 3 (a) J. Chieffari, Y. Chong, F. Ercole, J. Krstina, J. Jeffery, T. P. Le, R. T. Mayadunne, G. F. Meijis, C. L. Moad and G. Moad, *Macromolecules*, 1998, **31**, 5559–5562; (b) C. Boyer, V. Bulmus, T. P. Davis, V. Ladmiral, J. Q. Liu and S. Perrier, *Chem. Rev.*, 2009, **109**, 5402–5436; (c) D. J. Keddie, *Chem. Soc. Rev.*, 2014, **43**, 496–505; (d) B. Wenn, M. Conradi, A. D. Carreiras, D. M. Haddleton and T. Junkers, *Polym. Chem.*, 2014, **5**, 3053–3060; (e)



R. K. Bai, Y. Z. You and C. Y. Pan, *Macromol. Rapid Commun.*, 2001, **22**, 315–319; (f) L. Lu, H. J. Zhang, N. F. Yang and Y. L. Cai, *Macromolecules*, 2006, **39**, 3770–3776; (g) Z. Li, W. J. Chen, Z. B. Zhang, L. F. Zhang, Z. P. Cheng and X. L. Zhu, *Polym. Chem.*, 2015, **6**, 1937–1943; (h) Z. Li, W. J. Chen, L. F. Zhang, Z. P. Cheng and X. L. Zhu, *Polym. Chem.*, 2015, **6**, 5030–5035.

4 (a) A. J. D. Magenau, N. C. Strandwitz, A. Gennaro and K. Matyjaszewski, *Science*, 2011, **332**, 81–84; (b) N. Bortolamei, A. A. Isse, A. J. D. Magenau, A. Gennaro and K. Matyjaszewski, *Angew. Chem., Int. Ed.*, 2011, **50**, 11391–11394; (c) Y. Kwak and K. Matyjaszewski, *Macromolecules*, 2010, **43**, 5180–5183.

5 (a) T. Otsu and M. Yoshida, *Macromol. Rapid Commun.*, 1982, **3**, 127–132; (b) L. F. Fan, H. J. Jiang, L. F. Zhang, Z. P. Cheng and X. L. Zhu, *RSC Adv.*, 2015, **5**, 31657–31663.

6 (a) S. Shanmugam, J. Xu and C. Boyer, *J. Am. Chem. Soc.*, 2015, **137**, 9174–9185; (b) Y. G. Zhao, M. M. Yu, S. L. Zhang, Y. C. Liu and X. F. Fu, *Macromolecules*, 2014, **47**, 6238–6245; (c) X. L. Miao, W. Zhu, Z. B. Zhang, W. Zhang, X. L. Zhu and J. Zhu, *Polym. Chem.*, 2014, **5**, 551–557; (d) X. L. Miao, J. J. Li, Z. B. Zhang, Z. P. Cheng, W. Zhang, J. Zhu and X. L. Zhu, *Polym. Chem.*, 2014, **5**, 46414648; (e) X. D. Liu, L. F. Zhang, Z. P. Cheng and X. L. Zhu, *Polym. Chem.*, 2016, **7**, 3576–3588; (f) X. D. Liu, L. F. Zhang, Z. P. Cheng and X. L. Zhu, *Chem. Commun.*, 2016, **52**, 10850–10853; (g) Z. C. Huang, L. F. Zhang, Z. P. Cheng and X. L. Zhu, *Polymers*, 2017, **9**, 4; (h) T. G. McKenzie, Q. Fu, M. Uchiyama, K. Satoh, J. Xu, C. Boyer, M. Kamigaito and G. G. Qiao, *Adv. Sci.*, 2016, **3**, 1500394.

7 B. P. Fors and C. J. Hawker, *Angew. Chem., Int. Ed.*, 2012, **51**, 8850–8853.

8 (a) J. Xu, K. Jung, A. Atme, S. Shanmugam and C. Boyer, *J. Am. Chem. Soc.*, 2014, **136**, 5508–5519; (b) J. Xu, K. Jung and C. Boyer, *Macromolecules*, 2014, **47**, 4217–4229.

9 (a) S. Shanmugam, J. Xu and C. Boyer, *J. Am. Chem. Soc.*, 2015, **137**, 9174–9185; (b) S. Shanmugam, J. Xu and C. Boyer, *Chem. Sci.*, 2015, **6**, 1341–1349; (c) J. Xu, S. Shanmugam, H. T. Duong and C. Boyer, *Polym. Chem.*, 2015, **6**, 5615–5624; (d) S. Shanmugam, J. Xu and C. Boyer, *Angew. Chem., Int. Ed.*, 2016, **55**, 1036–1040; (e) S. Shanmugam, J. Xu and C. Boyer, *Polym. Chem.*, 2016, **7**, 6437–6449.

10 J. Zhu, X. L. Zhu, Z. P. Cheng, F. Liu and J. M. Lu, *Polymer*, 2002, **43**, 7037–7042.

11 M. Martiny, E. Steckhan and T. Esch, *Chem. Ber.*, 1993, **126**, 1671–1682.

12 E. Arceo, E. Montroni and P. Melchiorre, *Angew. Chem., Int. Ed.*, 2014, **53**, 12064–12068.

13 Q. Michaudel, V. Kottisch and B. P. Fors, *Angew. Chem., Int. Ed.*, 2017, DOI: 10.1002/anie.201701425.

14 (a) T. G. McKenzie, Q. Fu, E. H. H. Wong, D. E. Dunstan and G. G. Qiao, *Macromolecules*, 2015, **48**, 3864–3872; (b) B. Wenn and T. Junkers, *Macromolecules*, 2016, **49**, 6888–6895.

15 N. Corrigan, S. Shanmugam, J. Xu and C. Boyer, *Chem. Soc. Rev.*, 2016, **45**, 6165–6212.

16 (a) L. J. Bai, L. F. Zhang, J. L. Pan, J. Zhu, Z. P. Cheng and X. L. Zhu, *Macromolecules*, 2013, **46**, 2060–2066; (b) J. L. Pan, L. F. Zhang, L. J. Bai, Z. B. Zhang, H. Chen, Z. P. Cheng and X. L. Zhu, *Polym. Chem.*, 2013, **4**, 2876–2883.

